New digital techniques applied to A and Z identification using pulse shape discrimination of silicon detector current signals

S. Barlini, R. Bougault, P. Laborie, O. Lopez, D. Mercier, M. Pârlog, B. Tamain, E. Vient, E. Chevallier, A. Chbihi, et al.

New digital techniques applied to A and Z identification using Pulse Shape Discrimination of Silicon detector current signals.

S.Barlini [a,*], R.Bougault [a], Ph.Laborie [a], O.Lopez [a], D.Mercier [a], M.Parlog [a,d], B.Tamain [a], E.Vient [a], E.Chevallier [b], A.Chbihi [b], B.Jacquot [b], V.L.Kravchuk [c] for the FAZIA collaboration.

[a] *LPC Caen, ENSICAEN, University of Caen, CNRS/IN2P3, Caen, France*

[b] *GANIL, CEA/DSM-CNRS/IN2P3, Caen, France*

[c] *INFN-LNL, I-35020, Legnaro (Padova), Italy*

[d] *NIPNE, RO-76900, Bucharest, Romania*

Abstract

Extending Pulse Shape Discrimination (PSD) to digitized signals is one of the most promising methods to identify particles stopped in a detector. Using the CIME accelerator in the GANIL laboratory, a measurement campaign was done to collect data corresponding to different charges, masses and energies of implanted ions. These data are used to develop an algorithm capable to discriminate the different particles both in mass and charge. In this experiment, a 300 μm n-TD reverse mounted Si-Detector was used. These studies on PSD are part of the FAZIA R&D,

a research and development project aiming at building a new 4π array for isospin nuclear physics.

Key words: Pulse Shape Discrimination, PSA, Silicon detector, Current signal, PACI

PACS: 61.82.Fk,29.40.Wk, 84.30.Sk

1 Introduction

With respect to the first 4π arrays devoted to charged particles conceived in the 80's, progresses in detection apparatuses have permitted in the 90's the advent of compact 4π powerful devices [1] which allowed to improve the experimental study of the multifragmentation of highly excited nuclear systems, possibly connected to a first order phase transition in nuclear matter [2]. With the rapidly expanding number of Radioactive Ion Beam accelerators, the possibility is offered of studying also the isospin (N/Z) dependence of the Nuclear Equation of State (EOS). For this purpose, the range of the identified mass number A with a compact geometry has to be extended and low thresholds for A and Z identification are necessary; developments of techniques toward a third generation of 4π multidetectors are necessary [2]. One of the new proposed devices is FAZIA [3], a high granularity 4π apparatus for charged reaction products, planned to operate in the field of heavy-ion induced collisions below and around the Fermi energy (10-100 MeV/nucleon). FAZIA will be designed to study Thermodynamics and Dynamics of excited exotic nuclei, exploring for example the isospin, temperature and density de-

* barlini@fi.infn.it, ANR fellow

pendence of the EOS symmetry energy term [2]. In order to reach the best performances, this detector will exploit the development of digital electronics. In fact, by using high frequency Analog to Digital Converters, it is now possible to implement a fully digital processing of the signals produced by detected particles and perform (possibly on-line) identification by using Digital Signal Processor techniques. With such components which can be integrated in a compact way, one expects to be able to build new detectors with better angular resolution, better mass discrimination and lower identification thresholds. Using digital electronics, the mass number (A) and atomic number (Z) identification via Pulse Shape Discrimination (PSD) can be envisaged in a new and more complete approach. PSD is not a new technique (see, for example, [4] and the following studies in relation with its application inside a 4π silicon ball detector [5,6,7,8]), but as recent studies have demonstrated [9,10,11], we have now the possibility to perform it in a fully digital way. Through the PSD in the first detection layer, we will be able to decrease the identification threshold with respect to the standard ΔE-E telescope technique which requires that particles have enough energy to punch through the ΔE detector. Simplifying and automating the calibration procedure is also essential as the number of detectors is becoming larger and larger for highest granularity and angular coverage. In order to study and possibly improve PSD algorithms, a measurement campaign was performed using the CIME cyclotron in the GANIL laboratory. In this paper, we report on new results concerning the mass number identification of ions stopped in a Silicon detector by using Pulse Shape Analysis on the current signal. We found that, at energies around $E/A = 8MeV$, it is possible to fully identify the mass number for carbon isotopes, while from Argon up to Krypton isotopes, the mass number resolution can be considered,

at least for the moment, of about 2-3 mass units.

2 EXPERIMENTAL SETUP

The measurements were performed at GANIL using the ions accelerated by the CIME cyclotron. In this experiment we have decided to concentrate our attention on the current signal produced by the detected particle. The Si-Detector, collimated at 10 mm diameter, was mounted on a mechanical support and placed directly inside the beam line to collect the ions without the needs of any target. The detector used was a 300 μm thick n-TD silicon (200 mm_2 as active area) mounted in a reverse configuration (rear contact as entrance window and hence lower electric field). The shape of current signals from solid state detectors is mainly governed by the combination of plasma erosion time and charge carrier collection time effects. In contrast to front-side injection, the reverse-side configuration amplifies the plasma-time differences: for ions of a given energy, an enhanced dependence of the risetime and of the whole signal is expected and observed indeed when using reverse mount configuration([5],[12]). The applied voltage was fixed at a value of 190 V during the experiment, while the depletion voltage for this detector was 140 V. The energy of the beam was such that the ions were always stopped in the detector and the beam spot was of about 3 mm in diameter. The pre-amplifier used in the experiment was the low-gain-version of the PACI described in [9]: it provides two outputs, proportional to the charge and the current produced by the detected particle. It was mounted as close to the detector as possible (4 cm) inside the vacuum chamber. This solution will be applied also in the FAZIA project, to avoid signal degradation. The PACI current output was

sent to an ACQIRIS acquisition system [13], which is a commercial 8 bit digitizer sampling at 2 GHz. All the signals from the different ions were stored using the same amplitude scale on the ACQIRIS system, so they are directly comparable. The PACI charge output was sent to standard shaping analogue electronics to measure the energy with a peak-sensing ADC. In the following the energy measurements always refer to this kind of determination. The trigger was done using the fast output of the charge amplifier and a proper trigger logic permitted to acquire, for each event, both the whole current signal and the shaped energy from the peak-sensing ADC. The energy of the beam in the experiment varied from 7.39 $AMeV$ to 8.68 $AMeV$ and the species of accelerated ions covered a somewhat wide range, from ^{12}C up to ^{84}Kr. The cocktail beam measured energy in Fig. 1, for example, was obtained with a single mixed source and a given setting of the cyclotron. In these conditions the Argon intensity was mainly optimized, with many other elements present in smaller quantities. All of them have the same final velocity, provided that the effective charge to mass ratio remains the same. Several runs were done corresponding to different settings of the cyclotron. During our experiment, we were working with a "mixed" beam with known effective charge allowing a very good velocity resolution (of the order of few 10^{-3}), but the corresponding absolute value was only known within about $\pm$ 1%. In Fig.1, one can see the ADC spectrum where each peak corresponds to a different accelerated isotope, all having $q/A = 0.25$ and energy of $E/A = 8.68$ $AMeV$. For the following analysis in order to select different ions, on each energy peak we made an energy selection by imposing a cut centred on the most probable value (with $\pm$ 0.5%). It would be very interesting to work in the future at smaller incident energies and to explore the lower energy limit of the PSD method presented in this article.

3 ANALYSIS AND RESULTS

The first step of data analysis was the total energy ADC calibration (see Fig. 2) in order to determine the mass number of the detected particle. Knowing the effective charge and the composition of the mixed source, it was possible to identify the different ions present in each experimental run before applying the PSD technique. For this calibration, 22 points were used, corresponding to all the available ions and energies except for the Kr-ions which are affected by the Pulse Height Defect (PHD). Fig. 3 shows different signals from our database. Inside the database, it was possible to find 3 pairs of isotopes with quite similar total energy : ^{12}C at 98.54 MeV versus ^{13}C at 96.75 MeV; ^{36}Ar at 313.92 MeV versus ^{40}Ar at 312.88 MeV and ^{80}Kr at 688.43 MeV versus ^{84}Kr at 676.18 MeV. Their energies are different by 1.82%, 0.33% and 1.78% respectively. This can slightly affect the results shown in this paper, but all the methods tested in the following are strictly applied on the same selected groups of events, so that the relative comparison between them is not affected by this problem. The first attempt to obtain a mass discrimination was done by looking at the distribution of the most simple and easiest parameters to extract (see Fig. 4): the signal amplitude, the risetime (i.e. the time needed to raise from 10% up to 90% of the amplitude), the decay time (i.e. the time needed in the second part of the signal to decrease from 90% to 10% of the amplitude) - both last calculations using an interpolation of the signal in order to improve the time resolution (see [14]) - and the 'rising-slope' (i.e. the angular coefficient of the linear interpolation between the point of 10% and the point of 90% of the signal). In Table 1, we report the separation obtained for each tested method by fitting, for each pair of isotopes, the distribution of signal

amplitude, risetime, etc... with two gaussians. Starting from the parameters of these fits, we can define the Factor of Merit M ([15]) as:

$$M = \frac{|\mu_1 - \mu_2|}{(\sigma_1 + \sigma_2) * 2.35} \tag{1}$$

where μ_1 and μ_2 are the centroids and σ_1 and σ_2 are the standard deviations of the two gaussian fits corresponding to the selected pairs of Carbon, Argon and Krypton isotopes. With this definition, the better is the discrimination, the larger the Factor of Merit. Usually one assumes that satisfactory discrimination is obtained for M>0.75 (rejection ratios for one ion with respect to the other of 12.5:1, [15]). According to this criterion, Table 1 shows that signal amplitude gives good results for Carbon and Argon, but it is not completely satisfactory for Krypton. Therefore, the use of "richer" parameters (or correlations among them) is needed to have a better separation in particular between the Kr isotopes. High order moments of the time distribution of the current signal, which take into account the whole sampled signal -i.e. the whole information available-, will be used in the following. A first step in this direction was shown in [9], where the second moment m_2 of the time distribution of the current signal is used in order to separate two isotopes of carbon (^{12}C and ^{13}C) at 80 MeV. As one can see in Table 1, the m_2 method is not able to discriminate the heaviest ions. As we will explain in this paper, it is possible to improve this result by exploiting the correlation between the second and the third moment. In order to extract the samples $f[i]$ of the current signal for the numerical analysis, one has first to subtract the baseline, which is a slightly fluctuating quantity from one event to the other. For each event, i.e. for each sample sequence, the mean baseline is obtained by averaging the first 400 samples preceding the very onset of the signal. Therefore, starting from

the sampling $s[i]$ provided by the ACQIRIS system, we can define the current signal $f[i]$ as:

$$f[i] = s[i] - b \tag{2}$$

where b is the mean baseline. In the formulae (4)-(5), the signals are rescaled to start with the first sample at $t = 0$. There is also a conversion factor on the time axis of to have the samples i expressed in ns (as the sample frequency is 2 GHz). In order to have also the different moments of the distribution expressed in ns and to compact the scale, we have extracted the $1/k^{th}$ root for each high order moment. For convenience, we will label them as usual mathematical moments. By taking into account the modifications introduced in the calculation of the different moments of the signal, the formulae become:

$$m_0 = \sum_{i=istart}^{istop} f[i] \tag{3}$$

$$m_1 = \sum_{i=istart}^{istop} \frac{f[i](i - start)0.5}{m_0} \tag{4}$$

$$m_k = \left| \sum_{i=istart}^{istop} \frac{f[i]\left[0.5(i - start) - m_1\right]^k}{m_0} \right|^{1/k} \tag{5}$$

where i is the i^{th} sampling point of the signal. The sum is done between a start, that is the first sampling point where the signal is higher than the fixed threshold with respect to the mean baseline (i_{start}) and a stop, that is the sampling point where the signal becomes smaller than the same threshold (i_{stop}). The threshold thus defines the zone where the samples are assumed to correspond to real signals. Considering the strong asymmetry of our current signals, the averaged value of m_1 in the configuration $f[i]$ is not centred with respect to the time extension of the signal, while the higher order moments

defined by (5) are indeed "centred moments", i.e. they are calculated with respect to the distribution centroid. In order to study the discrimination efficiency of the moments method applied to a signal for which the m_1 will be more centred with respect to the time extension, we proceeded in the following way: we define another sequence ($data[i]$) related to the current signals:

$$data[i] = C_{baseline} - f[i] \tag{6}$$

where $C_{baseline}$ is a fixed constant for each pair of ions, greater than the amplitude of the analysed signal in order to keep always the signal completely positive (so that the meaning of moments is preserved). In the upper part of Fig.5, the averaged signals for the 3 pairs of ion are shown in configuration $f[i]$. In the bottom part of Fig.5, the m_1 distribution with the signal expressed as $data[i]$ with different values of $C_{baseline}$ is compared to the m_1 distribution with the signal expressed as $f[i]$. The use of $data[i]$ configuration and the variation of $C_{baseline}$ has various influences in the moment calculation. In fact, it changes the position of m_1, i.e. it varies the "centrality" of the moments. Moreover, since $data[i]$ is greater when $f[i]$ is smaller and vice versa, new weights are given to the various portions of the signal, namely the onset and the end of the signal have a higher influence on the so-calculated moments. As one can see in Table 2, by a proper selection of the constant $C_{baseline}$, we can find a value for which the averaged value of the m_1 is close to the middle of the duration time of the signal. Note that the m_1 distribution becomes also centred near the crossing point of the averaged signal corresponding to the different isotopes. These values of the constant $C_{baseline}$ are respectively around 100, 150 and 80 for Carbon, Argon and Kripton isotopes. Using $data[i]$ with the proposed value of $C_{baseline}$, we have a more equilibrated weight-sharing in

the calculation of the different moments between the two parts of the signal which are connected to the collection of the electrons (fast part of the signal) and the holes (slow part of the signal). This effect is more evident in the case of heavy ions, as Krypton, where the time duration of the current signal is longer and more asymmetric. Having verified that the distribution of a single moment (m_1, m_2, etc.) is not sufficient to provide the desired discriminations, we studied, for each ion pair at a given energy, the various correlations between two moments. From all the examined cases, it appears that the best discrimination approach in our case is to use the second vs. third moment correlation. Working in this bi-dimensional plane, it is possible to achieve the best separation between the 3 selected pairs of ions, as one can see in the example shown in Fig.6, refering to Ar-isotopes. Looking at Fig.6, one can see that the directions of the major axis of the m_2 vs m_3 correlation for ^{36}Ar and ^{40}Ar are almost parallel. We observe basically the same behaviour for the other analysed ion pairs. Therefore we can obtain a more efficient separation by projecting the bi-dimensional plot along a direction perpendicular to the direction of the two major-axes of the distributions ($x^{'}$ in the Fig.6), once the necessary rotation of variables is applied:

$$x^{'} = (m_2 - x_0)cos\alpha + (m_3 - y_0)sin\alpha \tag{7}$$

where α is the rotation angle between the old reference system (m_2, m_3) and the new reference system $(x^{'}, y^{'})$, while $O^{'}(x_0, y_0)$ is the new axis origin. After the projection, we can estimate the quality of the discrimination with the Factor of Merit M defined as before. In Figs. 7,8, one can see the projections corresponding to the 3 different pairs of ions ^{12}C vs ^{13}C, ^{36}Ar vs ^{40}Ar and ^{80}Kr vs ^{84}Kr using the $data[i]$ configuration with the value of $C_{baseline}$ which opti-

mizes the Factor of Merit. In Table 3 the values coming out from a gaussian fit on the peak of Fig.7 and Fig.8 are shown, while in Table 4 are reported the corresponding Factor of Merit M for the two signal configurations, the standard one ($f[i]$) and the proposed one ($data[i]$). The improvement in the discrimination is quite evident, especially in the case of Krypton. By comparing this moment correlation method with the other simpler techniques (Table 1), we observe that better results are always obtained, even reaching a satisfactory value of M=1.04 for the otherwise problematic case of Krypton. In Table 3 one can also see that, using $data[i]$, the Factor of Merit for Krypton is larger than for Argon. This is probably due to the fact that the current signals associated to Krypton are longer and more asymmetric than those of Argon. So that, the effect to use $data[i]$ instead of $f[i]$ is greater in the Krypton case with respect to the Argon case. In the light of the more recent measurement campaign performed by the FAZIA collaboration at the Laboratori Nazionali di Legnaro ([16], [17]), we should not forget that the $< 111 >$ Silicon detector used in the presently described experiment was not tilted, so that the presence of a not negligible fraction of events that have experienced the channelling effect in a such relevant way to change the shape of the current signal should be considered. The ions channelled along the crystal major axis or planes, in fact, are leading to signals with a different shape as compared to those induced by ions impinging along random directions ([17]). Concerning the PSD results presented in Figs. 7 and 8, we suspect that channelled ions maybe responsible for the left tail visible for Carbon and Argon isotopes. For Krypton (Fig.8) the effect is not appreciable because the energy selection was done in the same way as for the other ions ($\pm$ 0.5% with respect to the mean value), thus resulting in a more efficient way to remove a large fraction of the channelled ions: in fact, for heavy ions the "channelled" particles show a larger energy difference

with respect to the "random" ones ([17]), because the effect is mediated by Pulse Height Defect, increasing with ion charge for a given velocity.

4 CONCLUSION

Digital PSD is one of the most promising techniques to exploit when building new detectors with enhanced identification resolution. Through Digital PSD, it will be possible to decrease the identification threshold. Moreover, if one is able to perform the discrimination on-line, using fast on-board electronics, the following off-line calibration work can be also significantly reduced. In this paper, we have presented a new discrimination technique applied to the current signals produced in a n-TD Silicon detector by various heavy-ions fully stopped in the Silicon detector. The experiment was performed at GANIL in the early stage of the FAZIA collaboration. On the basis of the obtained Factor of Merit, one can say that the limit of the proposed technique is currently one mass unit separation in the region of Carbon ions and a separation of about 2-3 units of mass, in the Ar and Kr ion regions, for an energy of around E/A =8 $AMeV$. Other experiments have stressed the importance of carefully avoiding channeling effect ([16], [17]) and the necessity of using Silicon material with very uniform doping for PSD applications ([7],[18]). Taking into account these (partly new) results, the actual limit for the m_2 vs m_3 discrimination technique proposed in the article is expected to be prone for possible further improvements: one plans to verify this during the next experiments, where the problems concerning the channeling and the resistivity uniformity of the detector will be addressed and possibly solved. Using a wider mass and energy distribution (as plainned in the next R&D FAZIA experiments), we

hope to adress the low threshold problem, i.e. the limitation of PSA. The data presented here do not allow to conclude on this specific point. Apart from the obtained results, we stress again that an interesting characteristic of this discrimination technique is the possibility of calculating - directly "on line" - the high order moments values m_2 and m_3 of the time distribution of the signals. In this way, one may avoid to store the whole signal (with the associated problems of memory and data transfer) in order to obtain the mass and charge discrimination. The information will be condensed in some relevant parameters, allowing to build two-dimensional maps as the m_2 vs m_3 discussed in this article, together with other ones, as for example the charge risetime vs energy plot as alternative to the standard Time of Flight-Energy technique. The presented technique has to be tested in a "real" experiment and not only with mono-energetic known A and Z beam. With a large distribution of masses and energies it is possible that the proposed technique has to be coupled to a more standard technique for element identification before to be applied to the data set: first a Z-identification through Rise Time versus Energy and an optimal choise of $C_{baseline}$ for each element (Eq.6), and then (m_2,m_3)-A identification. Other works and more complete experiments are necessary to extend the ion database needed to improve and test this proposed PSD technique, which seems to be a very promising field of investigation.

5 ACKNOWLEDGMENTS

The authors wish to thank the LPC staff for the help in the preparation of the experiment and in particular J.F.Cam, Ph.Desrue, D.Etasse and Y.Merer. We want also to stress the important contribution given to the experiment by

all the GANIL staff, and in particular we want to cite E.Gueroult. Finally, the author wants to thank M.D'Agostino for her suggestions in the development of this discrimination technique and L.Bardelli. This work has been supported by the Agence Nationale de la Recherche under grant number ANR-05-BLAN-0373-01.

References

[1] A.Bonasera, M.Bruno, C.O.Dorso and P.F.Mastinu "Critical phenomena in nuclear fragmentation", Nuovo Cimento vol. 23, n.2 (2000)

[2] "Dynamics and Thermodynamics with Nuclear Degrees of Freedom" edited by Ph. Chomaz, F.Gulminelli, W.Trautman and S.J. Yennello, Eur. Phys. J. A30, III (2006)

[3] more information on http://fazia.in2p3.fr

[4] C.A.J. Ammerlaan, R.F.Rumphorst and A.Ch.Koerts, Nucl. Instr. and Meth. 22(1963), 189

[5] G.Paush, W.Bohne, D.Hilscher, Nucl. Instr. and Meth. A337(1994), 573

[6] G.Paush, H.-G.Ortlepp, W.Bohne, H.Grawe, D.Hilscher, M.Moszyński, D.Wolski, R.Schubart, G.de Angelis and M.de Poli, IEEE Trans. Nucl. Sci. NS-43(1996), 1097

[7] G.Paush, M.Moszyński, W.Bohne, J.Cederkäll, H.Grawe, W.Klamra, M.-O.Lampert, P.Rohr, R.Schubart, W.Seidel and D.Wolski, IEEE Trans. Nucl. Sci. NS-44(1997), 1040

[8] G.Paush, H.Prade, M.Sobiella, H.Schnare, R.Schwengner, L.Käubler, C.Borcan, H.-G.Ortlepp, U.Oehmichen, H.Grawe, R.Schubart,

J.Gerl, J.Cederkäll, A.Johnson, A.Kerek, W.Klamra, M.Moszyński, D.Wolski, M.Kapusta, A.Axelsson, M.Weiszflog, T.Härtlein, D.Pansegrau, G.de Angelis, S.Ashrafi, A.Likar, M.Lipoglavšek, Nucl. Instr. and Meth. A443(2000), 304

[9] H.Hamrita, E.Rauly, Y.Blumenfeld, B.Borderie, M.Chabot, P.Edelbruck, L.Lavergne, J.Le Bris, Th.Legou, N.Le Neindre, A.Richard, M.F.Rivet, J.A.Scarpaci, J.Tillier, S.Barbey, E.Becheva, F.Bocage, R.Bougault, R.Bzyl, B.Carniol, D.Cussol, P.Désesquelles, D.Etasse, E.Galichet, S.Grévy, D.Guinet, G.Lalu, G.Lanzalone, Ph.Lautesse, O.Lopez, G.Martinet, S.Pierre, G.Politi, E.Rosato, B.Tamain, E.Vient, Nucl.Instr. and Meth. A531(2004), 607

[10] L.Bardelli, M.Bini, G.Poggi, N.Taccetti, Nucl.Instr. and Meth. A491(2002), 244

[11] L.Bardelli, G.Poggi, M.Bini, G.Pasquali, N.Taccetti, Nucl. Phys. A746(2004), 272

[12] J.B.A. England, G.M.Field and T.R.Ophel, Nucl. Instr. and Meth. A280 (1989), 291

[13] see http://ACQIRIS.com

[14] L.Bardelli, G.Poggi, M.Bini, G.Pasquali, N.Taccetti, Nucl. Instr. and Meth. A521(2004), 480

[15] R.A.Winyard, J.E.Lutkin and G.W.McBeth, Nucl.Instr. and Meth. 95(1971), 141

[16] L.Bardelli, M.Bini, G.Casini, A.Nannini, G.Pasquali, S.Piantelli, G.Poggi, A.Stefanini, M.Cinausero, F.Gramegna, V.L.Kravchuk, C.Scian, M.Bruno, M.D'Agostino, E.Geraci, J.De Sanctis, P.Marini, G.Vannini, S.Barlini, R.Bougault, M.F.Rivet, J.M.Andujar, R.Berjillos, J.A.Dueñas, J.Flores, A.Becla, T.Kozik, F.Negoita, S.Velica for FAZIA collaboration, Annual Report of LNL 2006, 248

[17] L.Bardelli, M.Bini, G.Casini, G.Pasquali, G.Poggi, S.Barlini, A.Becla, R.Berjillos, B.Borderie, R.Bougault, M.Bruno, M.Cinausero, M.D'Agostino, J.De Sanctis, J.A.Dueñas, P.Edelbruck, E.Geraci, F.Gramegna, A.Kordyasz, T.Kozik, V.L.Kravchuk, L.Lavergne, P.Marini, A.Nannini, F.Negoita, A.Olmi, A.Ordine, S.Piantelli, E.Rauly, M.F.Rivet, E.Rosato, C.Scian, A.Stefanini, G.Vannini, S.Velica, M.Vigilante for the FAZIA collaboration, NIM submited

[18] L.Bardelli et al., to be published

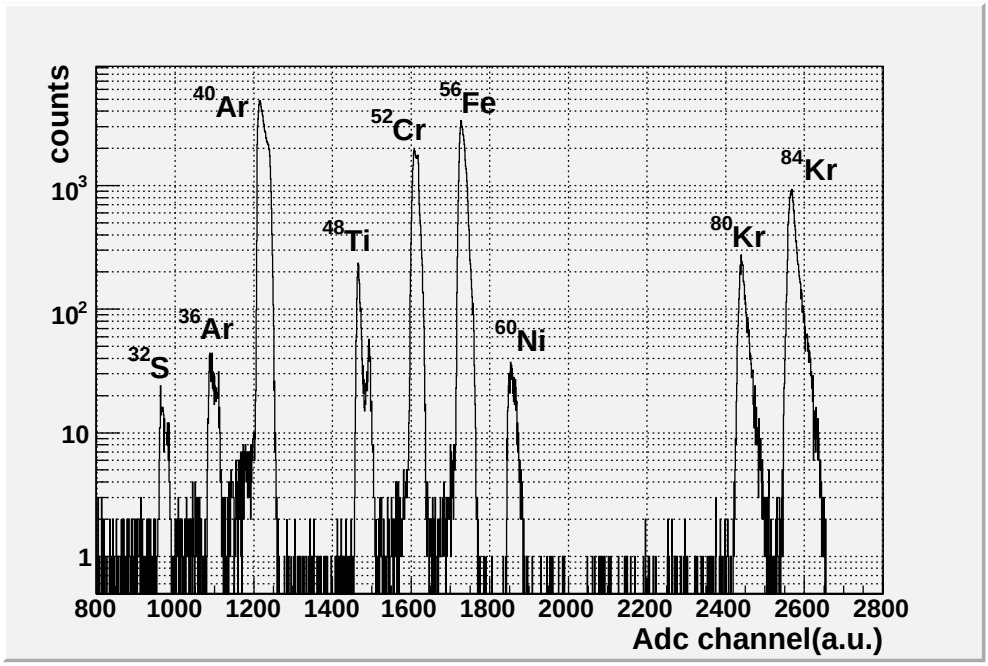

Fig. 1. ADC raw spectrum. One can see the different peaks corresponding to the different ions implanted in the detector (q/A=0.25).

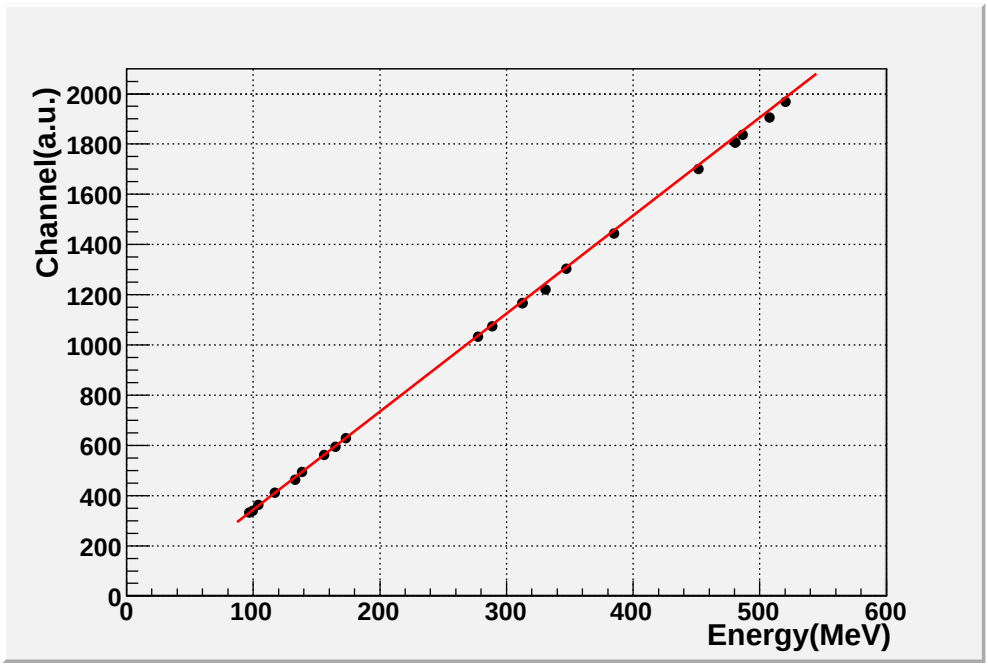

Fig. 2. Linear energy calibration of the ADC.

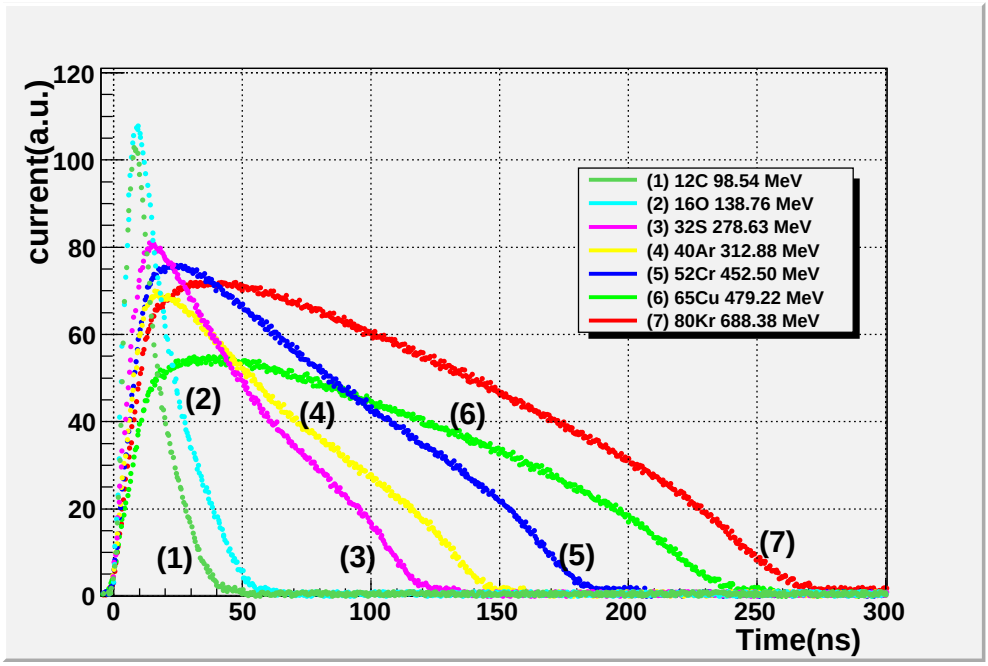

Fig. 3. Averaged signals (4000 events for each ion) corresponding to some ions of the database built after the CIME experiment.

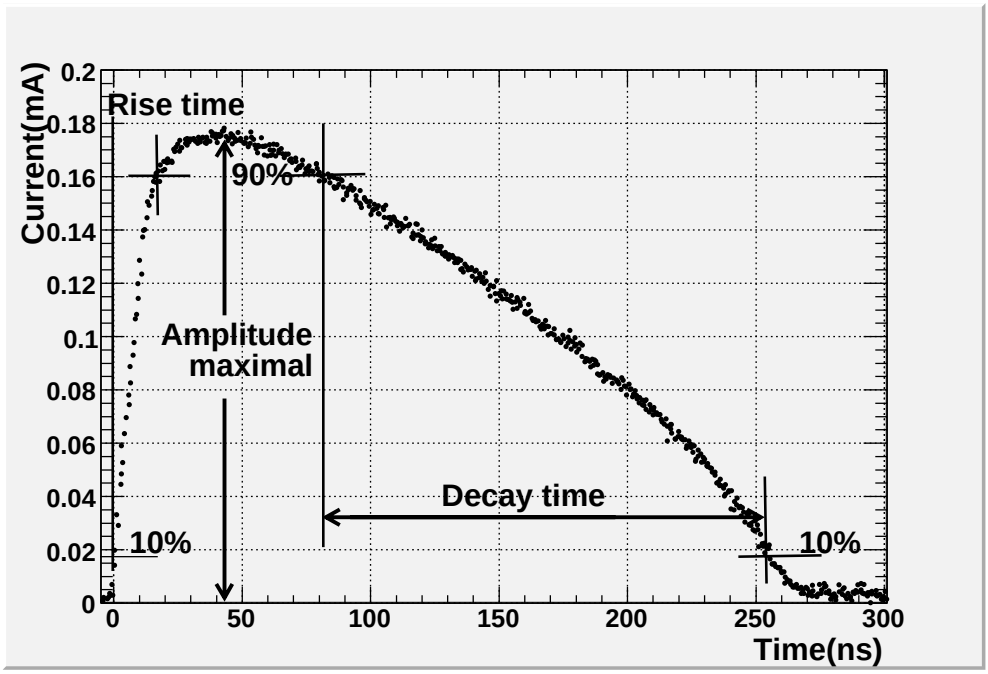

Fig. 4. Signal of ^{80}Kr@688 MeV on which one can easily see the definition of the risetime, decay time and signal amplitude.

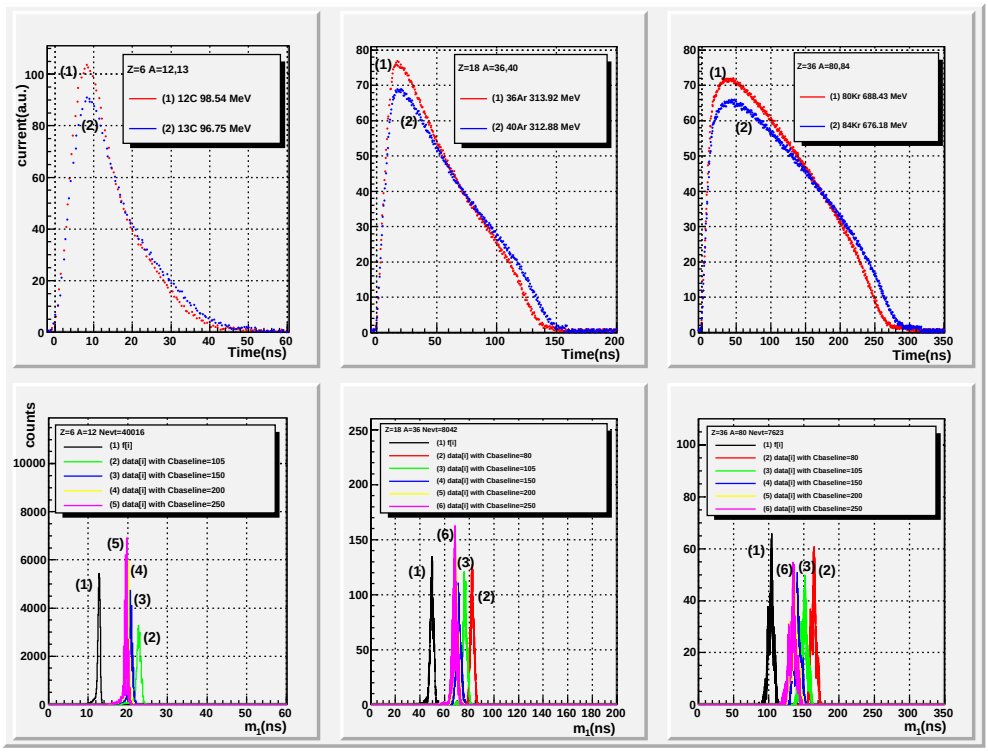

Fig. 5. Upper part: averaged signal for the 3 pairs of isotopes. Bottom part: m_1 distribution for the lighter isotope as a function of the signal configuration.

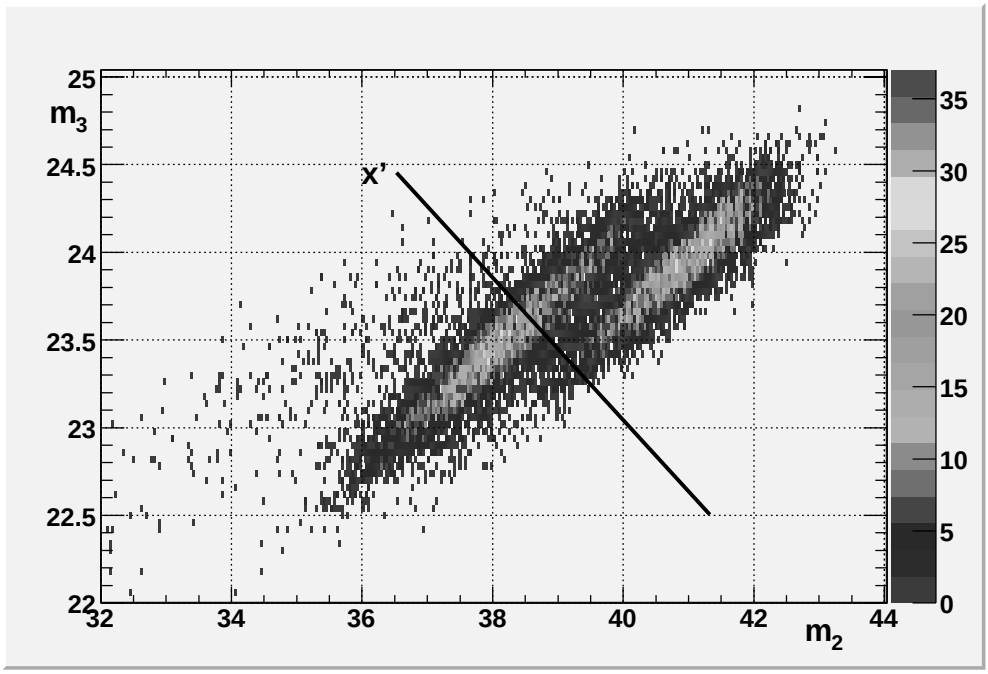

Fig. 6. Example of separation in the m_2 vs m_3 plane for Ar-isotopes.

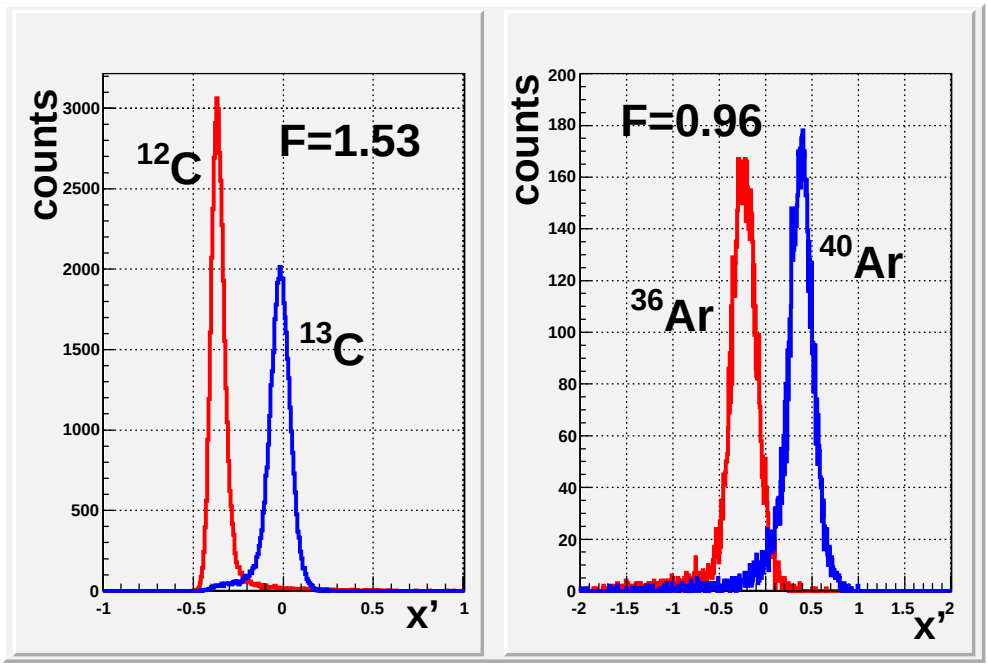

Fig. 7. Separation between ^{12}C vs^{13}C (left part) and ^{36}Ar vs^{40}Ar (right part) with the projection technique explained in the text.

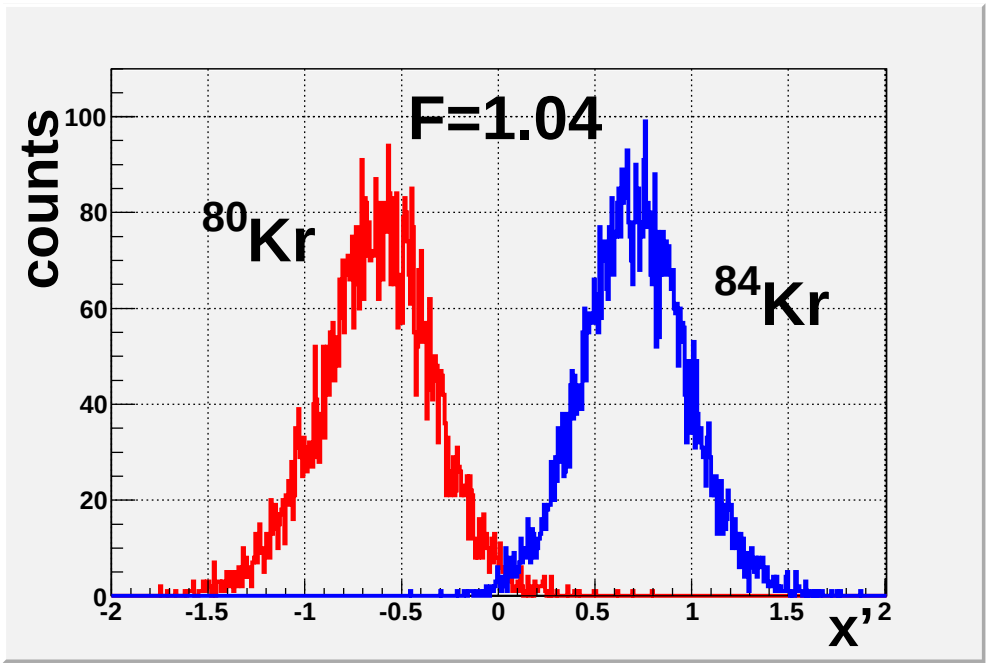

Fig. 8. Separation between ^{80}Kr vs^{84}Kr with the projection technique explained in the text.

Method	100 MeV ^{12}C, ^{13}C	312 MeV ^{36}Ar, ^{40}Ar	682 MeV ^{80}Kr, ^{84}Kr
Amplitude max. (mA)	M=1.42	M=0.81	M=0.54
Risetime (ns)	M=0.62	M=0.36	M=0.26
Decay time (ns)	M=0.81	M=0.48	M=0.07
Slope (mA/ns)	M=1.35	M=0.73	M=0.11
m_2 (ns)	M=0.91	M=0.64	$M = \sim 0$

Table 1

Merit Factor for the three pairs of ions ^{12}C vs ^{13}C, ^{36}Ar vs ^{40}Ar and ^{80}Kr vs ^{84}Kr using the "standard" discrimination methods (see text for details).

Couple of Ions	m_1 averaged using $f(i)$	m_1 averaged using $data(i)$	Signal extension
Carbon	12.8 ns	22.8 ns	45 ns
Argon	49.7 ns	71.2 ns	150 ns
Kripton	103.4 ns	164.2 ns	300 ns

Table 2

Averaged value of m_1 for ^{12}C, ^{36}Ar and ^{80}Kr using the signal in configuration f[i] and data[i] with the value of $C_{baseline}$ equal to 103, 155 and 83 respectively. They are compared with the extension time of the signal.

Couple of Ions	$Mean_1$	$Sigma_1$	$Mean_2$	$Sigma_2$
100 MeV ^{12}C+^{13}C	-0.361	0.036	-0.018	0.059
312 MeV ^{36}Ar+^{40}Ar	-0.231	0.134	0.380	0.138
682 MeV ^{80}Kr+^{84}Kr	-0.625	0.280	0.701	0.261

Table 3

Fit values from a Gaussian fit applied to the couples of peaks shown in Fig.7 and Fig.8.

Couple of Ions	Merit Factor using $f(i)$	Merit Factor using $data(i)$
100 MeV ^{12}C+^{13}C	1.15	1.53
312 MeV ^{36}Ar+^{40}Ar	0.84	0.96
682 MeV ^{80}Kr+^{84}Kr	0.50	1.04

Table 4

Table of Merit Factor for the four pairs of ions ^{12}C vs ^{13}C, ^{36}Ar vs ^{40}Ar, ^{80}Kr vs ^{84}Kr for the new discrimination method using $f(i)$ and $data(i)$ (see text for details).